MODELLING OF ACOUSTIC POWER RADIATION FROM MOBILE SCREW COMPRESSORS

Jan Dupal*[1], Jan Vimmr[1], Ondřej Bublík[1], Michal Hajžman[1]

[1]European Centre of Excellence NTIS - The New Technologies for Information Society,
Faculty of Applied Sciences, University of West Bohemia, Pilsen, Czech Republic
dupal@kme.zcu.cz
jvimmr@kme.zcu.cz
obublik@kme.zcu.cz
mhajzman@kme.zcu.cz

Keywords: Screw Compressor, Vibro-Acoustics, Helmholtz Equation, Finite Element Method.

Abstract. *The method for a numerical solution of the vibro-acoustic problem in a mobile screw compressor is proposed and the in-house 3D finite element (FE) solver is developed. In order to reduce the complexity of the problem, an attention is paid to the numerical solution of the acoustic pressure field in the compressor cavity interacting with linear elastic compressor housing. Propagation of acoustic pressure in the cavity is mathematically described by Helmholtz equation in the amplitude form and is induced by periodically varying surface velocity of the compressor engine which can be determined experimentally. Numerical solution of Helmholtz equation for acoustic pressure amplitude distibution inside the cavity with regards to prescribed boundary conditions is performed using FE method on unstructured tetrahedral grid. For the FE discretisation of the elastic compressor housing (modelled as a thin metal plate), a six-noded thin flat shell triangular finite element with 18 DOF based on the Kirchhoff plate theory was developed and implemented. The resulting strong coupled system of linear algebraic equations describing the vibro-acoustic problem, i.e. the problem of interaction between the air inside the cavity and the screw compressor housing, is solved numerically by well-known algorithms implemented in Matlab. The developed 3D FE solver is verified against the approximate analytical solution of a specially designed benchmark test case. A construction of the benchmark test analytical solution is also presented in the paper. The verified FE solver is applied to vibro-acoustic problem of the simplified model of a screw compressor and its numerical results, i.e. distribution of the acoustic pressure amplitudes in the cavity and absolute values of the compressor housing deflection amplitudes, are discussed.*

1 INTRODUCTION

Considering customer requirements and the necessity to satisfy hygienic standards, the producers of mobile screw compressors are compelled to minimise the emitted acoustic power and the related noise. The ongoing research is focused on a proposal of a suitable and efficient method and its implementation within an in-house computational software for the numerical solution of the acoustic power radiation from screw compressors. The knowledge from computational results will be used to alter the mobile screw compressor design so that the total emitted acoustic power is significantly decreased.

The solution of the above stated goals represents a complex problem. This paper is primarily focused on the numerical solution for the vibro-acoustic problem of the simplified model of the mobile screw-compressor. Main attention is paid to the acoustic pressure distribution [1, 2, 3, 4] in the compressor cavity interacting with the linear elastic housing of the screw compressor. It is assumed that the propagation of the acoustic pressure in the cavity is induced by periodically varying surface velocity of the compressor engine, which is known a priori (e.g. experimentally measured). Since the periodic function can be expressed in the form of Fourier series, the problem can be solved for a single frequency value and with regards to linearity of the problem the global solution can be derived using a superposition of the harmonic solutions. Based on this assumption, the acoustic pressure $p'(\boldsymbol{x}, t)$ and the acoustic velocity $\mathbf{v}'(\boldsymbol{x}, t)$ can be expressed in the complex harmonic form $p'(\boldsymbol{x}, t) = p(\boldsymbol{x})e^{i\omega t}$ and $\mathbf{v}'(\boldsymbol{x}, t) = \mathbf{v}(\boldsymbol{x})e^{i\omega t}$, respectively, where ω is an angular frequency of compressor engine movement.

The method used for numerical solution of the vibro-acoustic problem is implemented into a newly developed 3D finite element (FE) solver in Matlab. The FE solver is verified based on the approximate analytical solution of a specially designed benchmark test case. Furthermore the FE solver is applied to the vibro-acoustic problem in the simplified model of a screw compressor and its numerical results, i.e. distribution of the acoustic pressure amplitudes in the cavity and absolute values of the compressor housing deflection amplitudes, are discussed.

2 PROBLEM FORMULATION

In the following, the computational domain is divided into two regions, the compressor cavity $\Omega \subset \mathbf{R}^3$ and the elastic compressor housing $\tilde{\Omega} \subset \mathbf{R}^3$, as displayed in Figure 1. The cavity domain Ω is bounded by the boundary $\partial\Omega = \Gamma_{in} \cup \Gamma_{out} \cup \Gamma_w \cup \Gamma_t$ where Γ_{in}, Γ_{out} and Γ_w denote the inlet, the outlet and the rigid walls of the computational domain, respectively. The elastic housing $\tilde{\Omega}$ is bounded by boundary $\partial\tilde{\Omega} = \Gamma_f \cup \Gamma_u \cup \Gamma_t$ where Γ_f denotes the boundary with prescribed force loads and Γ_u denotes the boundary with prescribed displacement field. The interface between the two interacting domains, i.e. between the cavity Ω and the housing $\tilde{\Omega}$, is denoted as Γ_t.

Figure 1: Computational domain $(\Omega \cup \tilde{\Omega}) \subset \mathbf{R}^3$.

In the cavity domain Ω, the distribution of acoustic pressure $p(\boldsymbol{x})$ is described by the Helmholtz equation in the amplitude form [2, 4, 5]

$$k^2 p + \Delta p = 0 \qquad (1)$$

where $k = \frac{\omega}{c}$ is the wave number, c is the speed of sound and ω is the angular frequency of the engine motion. The weak solution of the Helmholtz equation is given as
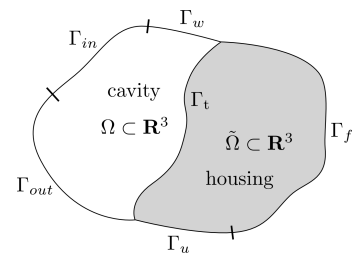
$$\int\limits_{\Omega} k^2 \varphi\, p\, \mathrm{d}\Omega - \int\limits_{\Omega} \nabla\varphi\nabla p\, \mathrm{d}\Omega + \int\limits_{\partial\Omega} \varphi\, \frac{\partial p}{\partial n}\, \mathrm{d}S = 0 \qquad (2)$$

where $\varphi(\boldsymbol{x})$ is a well chosen test function. The momentum conservation law for the inviscid fluid yields [2, 4]

$$\frac{\partial p}{\partial n} = -i\omega\varrho_a v_n \qquad (3)$$

where i is the imaginary unit, ϱ_a is the air density and $v_n = \boldsymbol{n}\cdot\boldsymbol{v}$ is the normal component of the acoustic velocity. The boundary condition $v_n = 0$ is prescribed at the rigid wall boundary Γ_w which yields $\int_{\Gamma_w} \varphi\, \frac{\partial p}{\partial n}\, \mathrm{d}S = -\int_{\Gamma_w} \varphi\, i\,\omega\varrho_a v_n\, \mathrm{d}S = 0$. The normal velocity v_n at the anechoic outlet Γ_{out} is given as $v_n = p/(\varrho_a c)$ [1, 4] which yields $\int_{\Gamma_{out}} \varphi\, \frac{\partial p}{\partial n}\, \mathrm{d}S = -\int_{\Gamma_w} \varphi\, i\, \frac{\omega}{c}\, p\, \mathrm{d}S$. For the inlet boundary Γ_{in} (i.e. the engine surface), the surface acoustic velocity v_n is prescribed. The interface Γ_t between the cavity and elastic housing holds $\int_{\Gamma_t} \varphi\, \frac{\partial p}{\partial n}\, \mathrm{d}S = -\int_{\Gamma_t} \varphi\, i\,\omega\varrho_a v_n\, \mathrm{d}S$, where the normal component of the acoustic velocity v_n is an unknown velocity resulting from the interaction between the acoustic environment in the cavity and the elastic housing of the screw compressor.

The solution in the housing domain $\tilde{\Omega}$ is based on the principle of virtual work (PVW) in the following form

$$\int\limits_{\tilde{\Omega}} \delta\boldsymbol{\varepsilon}^T\boldsymbol{\sigma}\, \mathrm{d}\tilde{\Omega} = -\int\limits_{\tilde{\Omega}} \varrho_h\delta\boldsymbol{u}^T\ddot{\boldsymbol{u}}\, \mathrm{d}\tilde{\Omega} + \int\limits_{\Gamma_t} p\,\delta\boldsymbol{u}^T\boldsymbol{n}\, \mathrm{d}S \qquad (4)$$

where $\boldsymbol{\varepsilon} = [\varepsilon_x, \varepsilon_y, \varepsilon_z, \gamma_{yz}, \gamma_{xz}, \gamma_{xy}]^T$ is the strain vector, $\boldsymbol{\sigma} = [\sigma_x, \sigma_y, \sigma_z, \tau_{yz}, \tau_{xz}, \tau_{xy}]^T$ is the stress vector, $\boldsymbol{u} = [u, v, w]^T$ is the displacement vector and ϱ_h is the material density of the housing. The surface integrals over the boundary Γ_u with prescribed zero displacements and Γ_f with prescribed zero loads are equal to zero and are therefore omitted from Eq. 4.

## 3   FINITE ELEMENT METHOD DISCRETISATION

The finite element discretisation of the cavity domain $\Omega \subset \mathbf{R}^3$ is carried out for an unstructured tetrahedral mesh, a sample tetrahedral element is shown in Figure 2(left). The amplitudes of the acoustic pressure and the acoustic velocity are approximated linearly as

$$p(\xi,\eta,\zeta) = \boldsymbol{\Phi}(\xi,\eta,\zeta)\mathbf{X}_e\mathbf{S}_e^{-1}\mathbf{p}_e\,, \qquad v_\nu(\xi,\eta,\zeta) = \boldsymbol{\Phi}(\xi,\eta,\zeta)\mathbf{X}_e\mathbf{S}_e^{-1}\mathbf{v}_\nu^e\,, \ \nu\in\{x,y,z\}\,, \quad (5)$$

where $\boldsymbol{\Phi}(\xi,\eta,\zeta) = [1,\xi,\eta,\zeta]$, $\mathbf{p}_e = [p_1,p_2,p_3,p_4]^T$ is the vector of the acoustic pressure amplitudes at each node of the finite element, Figure 2(left), and $\mathbf{v}_\nu^e = [v_{\nu 1}, v_{\nu 2}, v_{\nu 3}, v_{\nu 4}]^T$, $\nu\in\{x,y,z\}$ is the vector of ν-th components of the acoustic velocity amplitudes at each node of the finite element. The matrices $\mathbf{S}_e$ and $\mathbf{X}_e$ are of the following form

$$\mathbf{S}_e = \begin{bmatrix} 1 & x_1 & y_1 & z_1 \\ 1 & x_2 & y_2 & z_2 \\ 1 & x_3 & y_3 & z_3 \\ 1 & x_4 & y_4 & z_4 \end{bmatrix}, \qquad \mathbf{X}_e = \begin{bmatrix} 1 & x_1 & y_1 & z_1 \\ 0 & \bar{x}_2 & \bar{y}_2 & \bar{z}_2 \\ 0 & \bar{x}_3 & \bar{y}_3 & \bar{z}_3 \\ 0 & \bar{x}_4 & \bar{y}_4 & \bar{z}_4 \end{bmatrix}, \qquad (6)$$

while $\bar{x}_i = x_i - x_1$, $\bar{y}_i = y_i - y_1$, $\bar{z}_i = z_i - z_1$ for $i = 2,3,4$. The test function $\varphi(\xi,\eta,\zeta)$ is approximated linearly, similarly to the amplitudes of the acoustic pressure and the acoustic
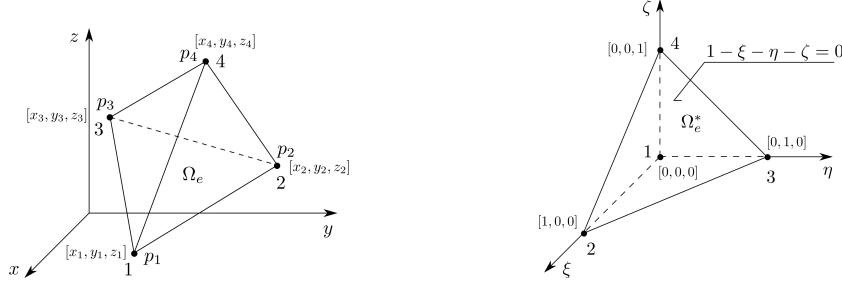
Figure 2: Tetrahedral finite element Ω_e (left) and normalised finite element Ω_e^* (right).

velocity. Substituting the approximations of the test function and of the acoustic pressure and velocity amplitudes, Eq. 5, into the weak solution given by Eq. 2 and taking the boundary integrals into consideration, we obtain a system of linear algebraic equations

$$\omega^2 \underbrace{\frac{|J_e|}{c^2}\mathbf{S}_e^{-T}\mathbf{X}_e^T\mathbf{A}_0\mathbf{X}_e\mathbf{S}_e^{-1}}_{\mathbf{H}_e}\mathbf{p}_e - \underbrace{\frac{1}{6|J_e|}\mathbf{S}_e^{-T}\mathbf{X}_e^T\mathbf{L}^T\mathbf{D}_e^T\mathbf{D}_e\mathbf{L}\mathbf{X}_e\mathbf{S}_e^{-1}}_{\mathbf{G}_e}\mathbf{p}_e - \tag{7}$$

$$-i\omega \underbrace{\frac{|J_{ej}^*|}{c}\mathbf{S}_e^{-T}\mathbf{X}_e^T\tilde{\mathbf{A}}_j\mathbf{X}_e\mathbf{S}_e^{-1}}_{\mathbf{F}_e}\mathbf{p}_e - i\omega\varrho_a \underbrace{|J_{ej}^*|\mathbf{S}_e^{-T}\mathbf{X}_e^T\mathbf{A}_j\mathbf{T}_e\mathbf{P}}_{\mathbf{C}_e^t}\mathbf{v}_e = i\omega\varrho_h \underbrace{|J_{ej}^*|\mathbf{S}_e^{-T}\mathbf{X}_e^T\mathbf{A}_j\mathbf{T}_e\mathbf{P}}_{\mathbf{C}_e^{in}}\mathbf{v}_e$$

where the matrices $\mathbf{H}_e$ and $\mathbf{G}_e$ are computed for all inner elements of the cavity domain Ω and the matrices $\mathbf{F}_e$, $\mathbf{C}_e^t$ and $\mathbf{C}_e^{in}$ are computed for the boundary elements at the boundaries Γ_{out}, Γ_t and Γ_{in}, respectively, see Figure 1. The matrix $\mathbf{L} = \left[\frac{\partial\boldsymbol{\Phi}^T}{\partial\xi}, \frac{\partial\boldsymbol{\Phi}^T}{\partial\eta}, \frac{\partial\boldsymbol{\Phi}^T}{\partial\zeta}\right]^T$, the matrices $\mathbf{D}_e$ and $\mathbf{T}_e$ are of the following form

$$\mathbf{D}_e = \begin{bmatrix} \bar{y}_3\bar{z}_4 - \bar{z}_3\bar{y}_4 & \bar{z}_2\bar{y}_4 - \bar{y}_2\bar{z}_4 & \bar{y}_2\bar{z}_3 - \bar{z}_2\bar{y}_3 \\ \bar{z}_3\bar{x}_4 - \bar{x}_3\bar{z}_4 & \bar{x}_2\bar{z}_4 - \bar{z}_2\bar{x}_4 & \bar{z}_2\bar{x}_3 - \bar{x}_2\bar{z}_3 \\ \bar{x}_3\bar{y}_4 - \bar{y}_3\bar{x}_4 & \bar{y}_2\bar{x}_4 - \bar{x}_2\bar{y}_4 & \bar{x}_2\bar{y}_3 - \bar{y}_2\bar{x}_3 \end{bmatrix}, \quad \mathbf{T}_e = \begin{bmatrix} \mathbf{X}_e\mathbf{S}_e^{-1} & \mathbf{0} & \mathbf{0} \\ \mathbf{0} & \mathbf{X}_e\mathbf{S}_e^{-1} & \mathbf{0} \\ \mathbf{0} & \mathbf{0} & \mathbf{X}_e\mathbf{S}_e^{-1} \end{bmatrix}, \tag{8}$$

$\mathbf{P}$ is the permutation matrix that changes the sequence of the FE parameters, $|J_e| = |\det \mathbf{J}_e|$ where $J_e = \bar{x}_2\bar{y}_3\bar{z}_4 - \bar{x}_2\bar{y}_4\bar{z}_3 - \bar{x}_3\bar{y}_2\bar{z}_4 + \bar{x}_3\bar{y}_4\bar{z}_2 + \bar{x}_4\bar{y}_2\bar{z}_3 - \bar{x}_4\bar{y}_3\bar{z}_2$, $|J_{ej}^*|$ expresses twice the area of each face of tetrahedral element, $\mathbf{A}_0 = \int\limits_0^1 \int\limits_0^{1-\xi} \int\limits_0^{1-\xi-\eta} \boldsymbol{\Phi}^T(\xi,\eta,\zeta)\boldsymbol{\Phi}(\xi,\eta,\zeta)\,\mathrm{d}\zeta\,\mathrm{d}\eta\,\mathrm{d}\xi$, the matrices $\tilde{\mathbf{A}}_j$, $j = 1, 2, 3, 4$ are obtained from the integration of the product of base functions $\boldsymbol{\Phi}(\xi,\eta,\zeta)$ over each face of the normalised tetrahedral element, Figure 2(right), and the matrices $\mathbf{A}_j$, $j = 1, 2, 3, 4$ are obtained from the integration of the product of base function matrices for the test function and for the normal velocity over each face of the normalised tetrahedral element. After dividing Eq. 7 by the term $(-i\omega)$ and after assembling the global matrices, the following equation is obtained

$$\frac{1}{\varrho_a}\left(i\omega\mathbf{H} + \frac{1}{i\omega}\mathbf{G} + \mathbf{F}\right)\mathbf{p} + \mathbf{C}^t\mathbf{v}^t = -\mathbf{C}^{in}\mathbf{v}^{in} \tag{9}$$

where $\mathbf{v}^{in}$ is the vector of prescribed acoustic velocity amplitudes in the element nodes located at the engine surface Γ_{in} and $\mathbf{v}^t$ is the vector of unknown acoustic velocity amplitudes in the element nodes located at the interface Γ_t.
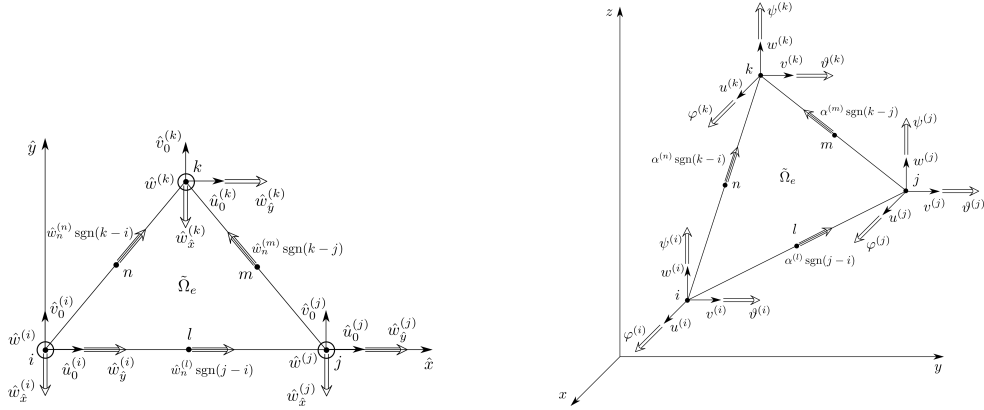
4

Figure 3: Six-noded thin flat shell triangular finite element $\tilde{\Omega}_e$ before (left) and after (right) transformation.

For the FE discretisation of the housing domain $\tilde{\Omega} \subset \mathbf{R}^3$, a new 6-noded thin flat shell triangular finite element with 18 degrees of freedom (DOF) was developed, see Figure 3(left). This thin flat shell element is based on the Kirchhoff plate theory. Each corner node i, j and k contains three displacements $\hat{u}_0$, $\hat{v}_0$, $\hat{w}$ and two rotations $\hat{w}_{\hat{x}}$, $\hat{w}_{\hat{y}}$. The mid-side nodes l, m and n store the information about normal derivatives of deflection $\hat{w}_n^{(l)}$, $\hat{w}_n^{(m)}$, $\hat{w}_n^{(n)}$, where the sense of rotation is determined by the sign of difference of numbers of the corresponding edge corner nodes, see Figure 3(left). Applying the PVW Eq. 4, the equation of motion for a housing element in the amplitude form is obtained with regards to a local coordinate system $(\hat{x}, \hat{y}, \hat{z})$ of the element as

$$i\omega \mathbf{M}_e \mathbf{v}_e^h + \mathbf{B}_e \mathbf{v}_e^h + \frac{1}{i\omega} \mathbf{K}_e \mathbf{v}_e^h + \mathbf{Q}_e \mathbf{p}_e = \mathbf{0} \,, \tag{10}$$

where $\mathbf{M}_e$ and $\mathbf{K}_e$ are the derived mass and stiffness matrices of the 6-noded thin flat shell triangular finite element, $\mathbf{B}_e = \beta \mathbf{K}_e$ is the proportional-damping matrix and $\mathbf{v}_e^h$ is the vector of velocity amplitudes for the nodes located in the housing of the screw compressor. The matrix $\mathbf{Q}_e$ expresses the distribution of acoustic pressure amplitudes at the element $\tilde{\Omega}_e$. In order to assembly the global matrices of mass $\mathbf{M}$, stiffness $\mathbf{K}$ and proportional-damping $\mathbf{B}$ and the global loading vector $\mathbf{Qp}$, it is necessary to perform a transformation of all matrices and vectors from the local coordinate system of the element $(\hat{x}, \hat{y}, \hat{z})$ to the global coordinate system (x, y, z). This way, two rotations $\hat{w}_{\hat{x}}$, $\hat{w}_{\hat{y}}$ at each corner node i, j and k of the element are transformed into three rotations φ, ϑ, ψ in the global coordinate system (x, y, z), while the rotations in the mid-side nodes l, m and n are not transformed, i.e. $\hat{w}_n^{(l)} \mathrm{sgn}(j - i) \equiv \alpha^{(l)} \mathrm{sgn}(j - i)$, $\hat{w}_n^{(m)} \mathrm{sgn}(k - j) \equiv \alpha^{(m)} \mathrm{sgn}(k - j)$ and $\hat{w}_n^{(n)} \mathrm{sgn}(k - i) \equiv \alpha^{(n)} \mathrm{sgn}(k - i)$. The displacements $\hat{u}_0$, $\hat{v}_0$, $\hat{w}$ in the corner nodes i, j and k of the element are transformed into displacements u, v, w. Using this transformation the obtained finite element has 21 DOF, as shown in Figure 3(right). The resulting matrix equation describing the motion of the compressor's housing in the global coordinate system (x, y, z) yields

$$i\omega \mathbf{M} \mathbf{v}^h + \mathbf{B} \mathbf{v}^h + \frac{1}{i\omega} \mathbf{K} \mathbf{v}^h + \mathbf{Q} \mathbf{p} = \mathbf{0}. \tag{11}$$

The vector of acoustic velocity amplitudes $\mathbf{v}^h$ can be divided into the subvector of velocity amplitudes $\mathbf{v}^t$ of compressor housing nodes at the interface Γ_t and into the subvector of velocity amplitudes $\mathbf{v}^{\tilde{\Omega}}$ of the other nodes inside the compressor housing domain $\tilde{\Omega}$. Thus the coefficient

matrices **M**, **B**, **K** can be divided into dedicated blocks and Eqs. (9), (11) can be rewritten as

$$
\begin{bmatrix}
\frac{1}{\varrho_a}\left(i\omega\mathbf{H}+\frac{1}{i\omega}\mathbf{G}+\mathbf{F}\right) & \mathbf{0} & \mathbf{C}^t \\
\mathbf{0} & i\omega\mathbf{M}_{11}+\mathbf{B}_{11}+\frac{1}{i\omega}\mathbf{K}_{11} & i\omega\mathbf{M}_{12}+\mathbf{B}_{12}+\frac{1}{i\omega}\mathbf{K}_{12} \\
\mathbf{Q} & i\omega\mathbf{M}_{21}+\mathbf{B}_{21}+\frac{1}{i\omega}\mathbf{K}_{21} & i\omega\mathbf{M}_{22}+\mathbf{B}_{22}+\frac{1}{i\omega}\mathbf{K}_{22}
\end{bmatrix}
\cdot
\begin{bmatrix}
\mathbf{p} \\
\mathbf{v}^{\tilde{\Omega}} \\
\mathbf{v}^t
\end{bmatrix}
=
\begin{bmatrix}
-\mathbf{C}^{in}\mathbf{v}^{in} \\
\mathbf{0} \\
\mathbf{0}
\end{bmatrix} . \quad (12)
$$

The resulting strong coupled system of linear algebraic equations describing the vibro-acoustic problem, i.e. the problem of interaction between the air inside the cavity Ω and the elastic housing $\tilde{\Omega}$, is solved numerically by well-known algorithms implemented in Matlab.

4 ANALYTICAL SOLUTION OF THE VIBRO-ACOUSTIC PROBLEM

In order to verify the method described above and to validate numerical results of the developed solver, a benchmark test case, which can be solved analytically, is suggested.

For simplicity, a rectangular cavity domain $\Omega \subset \mathbf{R}^2$ with dimensions $a \times b$ is considered. The amplitude of normal velocity $v_n^{in}(x) = A_0 \sin\frac{2\pi x}{b}$ is prescribed at the boundary Γ_{in} at the bottom of the cavity domain and normal velocity $v_n = 0$ is prescribed at the rigid side walls Γ_w. At the top of the cavity, there is a simple supported elastic beam $\tilde{\Omega} \subset \mathbf{R}^1$. Between the cavity and the elastic beam, there is the interface boundary Γ_t. The test setup is displayed in Figure 4. It is possible to find an approximate analytic solution of this simple vibro-acoustic problem describing the distribution of the acoustic pressure amplitudes in domain Ω and the deflection amplitudes in domain $\tilde{\Omega}$.
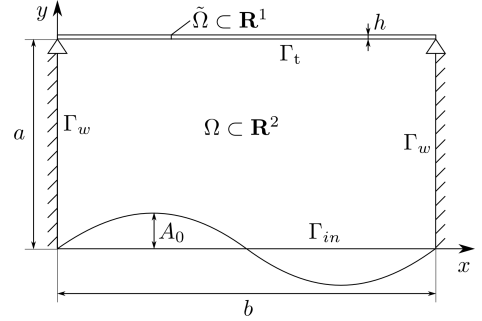

Figure 4: Computational domains $\Omega \subset \mathbf{R}^2$ and $\tilde{\Omega} \subset \mathbf{R}^1$ for the benchmark test case.

In this case, the weak solution of Eq. 1 for acoustic pressure amplitudes is

$$
\int_0^b \int_0^a \frac{\omega^2}{c^2}\varphi\, p \,\mathrm{d}y\mathrm{d}x - \int_0^b \int_0^a \nabla\varphi\nabla p \,\mathrm{d}y\mathrm{d}x + \int_{\Gamma_{in}\cup\Gamma_w\cup\Gamma_t} \varphi \frac{\partial p}{\partial n} \,\mathrm{d}s = 0 \quad (13)
$$

where $\varphi = \varphi(x,y)$ are well-chosen test functions. It is assumed, that the solution for the amplitude of the acoustic pressure can be approximated by finite series

$$
p(x,y) = \sum_{k=1}^{N}\sum_{l=1}^{N}\left(a_{kl}\sin\frac{k\pi x}{b}\sin\frac{l\pi y}{a} + b_{kl}\cos\frac{k\pi x}{b}\sin\frac{l\pi y}{a} + \right. \quad (14)
$$
$$
\left. +c_{kl}\sin\frac{k\pi x}{b}\cos\frac{l\pi y}{a} + d_{kl}\cos\frac{k\pi x}{b}\cos\frac{l\pi y}{a}\right)
$$

where N is a number of considered harmonics in x and y directions. With regards to Eq. 3, the following conditions are applied at the rigid wall boundary Γ_w

$$
\frac{\partial p}{\partial n} = -i\omega\varrho_a v_n = 0 \quad\Longrightarrow\quad \frac{\partial p}{\partial x}(0,y) = \frac{\partial p}{\partial x}(b,y) = 0 . \quad (15)
$$

Thus the a_{kl} and c_{kl} terms must be excluded from Eq. 14. The final form of the approximate solution for the acoustic pressure amplitudes is then

$$p(x,y) = \sum_{k=1}^{N}\sum_{l=1}^{N}\left(b_{kl}\underbrace{\cos\frac{k\pi x}{b}\sin\frac{l\pi y}{a}}_{\varphi_{kl}(x,y)} + d_{kl}\underbrace{\cos\frac{k\pi x}{b}\cos\frac{l\pi y}{a}}_{\varphi_{kl}^{\star}(x,y)}\right). \tag{16}$$

Due to the fact that Eq. 1 is of second order, the boundary conditions $\frac{\partial p}{\partial n}$ are unstable and the solution must be from a function space where $\int_0^b \int_0^a \varphi_{kl}(x,y)\,\mathrm{d}y\mathrm{d}x = \int_0^b \int_0^a \varphi_{kl}^{\star}(x,y)\,\mathrm{d}y\mathrm{d}x = 0$, which are the functions with null mean values. The function in Eq. 16 meets this requirement. The boundary integral over Γ_w from Eq. 13 is omitted with regards to Eq. 15. The velocity v_n at the boundary Γ_{in} is prescribed. Thus the term $\frac{\partial p}{\partial n}$ is given according to Eq. 3. At the interface Γ_t, the velocity v_n is identical for both the cavity domain Ω and the elastic beam $\tilde{\Omega}$. The amplitude of the elastic beam deflection is assumed to be the harmonic function

$$w(x) = \sum_{j=1}^{N}\alpha_j \sin\frac{j\pi x}{b} \tag{17}$$

which yields the amplitude of velocity of the beam

$$v(x) = i\omega\sum_{j=1}^{N}\alpha_j \sin\frac{j\pi x}{b}. \tag{18}$$

In the following, the Galerkin method is applied. The estimated aproximate solution Eq. 16 is substituted into Eq. 13 and the functions $\varphi_{kl}(x,y)$, $\varphi_{kl}^{\star}(x,y)$ respectively, are applied as the test functions. This yield to two systems of N^2 algebraic equations for unknown coefficients b_{kl} and d_{kl}, $k,l = 1,\ldots,N$. Due to the fact that $\varphi_{kl}(x,0) = \varphi_{kl}(x,a) = 0$ the first system holds

$$\frac{\omega^2}{c^2}\int_0^b\int_0^a \varphi_{kl}(x,y)p(x,y)\,\mathrm{d}y\mathrm{d}x - \int_0^b\int_0^a \nabla\varphi_{kl}(x,y)\nabla p(x,y)\,\mathrm{d}y\mathrm{d}x = 0. \tag{19}$$

The second system is given as

$$\frac{\omega^2}{c^2}\int_0^b\int_0^a \varphi_{kl}^{\star}(x,y)p(x,y)\,\mathrm{d}y\mathrm{d}x - \int_0^b\int_0^a \nabla\varphi_{kl}^{\star}(x,y)\nabla p(x,y)\,\mathrm{d}y\mathrm{d}x + \tag{20}$$

$$+\omega^2\varrho_a\cos l\pi\sum_{j=1}^{N}\alpha_j\frac{b}{\pi}\frac{2j}{j^2-k^2}\Delta_{jk} = -\frac{i}{\omega}A_0\left[\frac{4b}{\pi(4-k^2)}\Delta_{2k}\right]$$

where $\Delta_{jk} = 1$ for $(j-k)$ even and $\Delta_{jk} = 0$ for $(j-k)$ odd. When considering the ortogonality of functions $\varphi_{kl}(x,y)$ and $\varphi_{kl}^{\star}(x,y)$, Eqs. (19-20) become significantly simplified.

The solution for the elastic beam $\tilde{\Omega} \subset \mathbf{R}^1$ is given below. With regards to Eq. 16, the acoustic pressure amplitude that is acting on the beam can be expressed in the form

$$p(x,a) = \sum_{k=1}^{N}\sum_{l=1}^{N}d_{kl}\cos\frac{k\pi x}{b}\cos l\pi. \tag{21}$$

The amplitude form of the elastic beam equation of motion can be written as

$$EI\frac{\partial^4 w}{\partial x^4} - \omega^2\varrho_h S\frac{\partial^2 w}{\partial t^2} = p(x,a) \tag{22}$$

where $I = \frac{h^3}{120}$ and $S = 0.1\, h$. After substituting Eq. 17 and Eq. 21 into Eq. 22, consequent multiplication by the term $\sin\frac{j\pi x}{b}$, $j = 1, \ldots, N$ and after integration over domain $\tilde{\Omega}$ (i.e. for $x \in \langle 0; b \rangle$), the following system of equations is derived

$$\alpha_j \frac{b}{2}\left(EI\frac{j^4\pi^4}{b^4} - \omega^2 \varrho_h S\right) = \sum_{k=1}^{N}\sum_{l=1}^{N} d_{kl} \cos l\pi\, \frac{b}{\pi}\frac{2j}{j^2-k^2}\Delta_{jk}. \tag{23}$$

Systems of Eqs. (19), (20) and (23) form a system of $2N^2 + N$ linear algebraic equations for $2N^2 + N$ unknown coefficients b_{kl}, d_{kl} and α_j where $j, k, l = 1, \ldots, N$. The system can be written in a block form

$$\begin{bmatrix} \mathbf{A}_{11} & \mathbf{A}_{12} & \mathbf{0} \\ \mathbf{A}_{21} & \mathbf{A}_{22} & \mathbf{A}_{23} \\ \mathbf{0} & \mathbf{A}_{32} & \mathbf{A}_{33} \end{bmatrix} \cdot \begin{bmatrix} \mathbf{b} \\ \mathbf{d} \\ \boldsymbol{\alpha} \end{bmatrix} = \begin{bmatrix} \mathbf{0} \\ \mathbf{c}_2 \\ \mathbf{0} \end{bmatrix} \tag{24}$$

where vectors $\mathbf{b}$, $\mathbf{d}$ and $\boldsymbol{\alpha}$ include unknown coefficients b_{kl}, d_{kl} and α_j, respectively. Substituting coefficients b_{kl}, d_{kl} and α_j into Eqs. (16-18) yields the solution for the acoustic pressure amplitudes in the cavity and for amplitudes of elastic beam deflections and velocities.

5 ANALYTICAL AND NUMERICAL RESULTS

First, results of the approximate analytical solution for the benchmark test case of section 4 are presented and a comparison with numerical results of the in-house developed 3D FE solver is provided. In order to test the performance of the new thin flat shell triangular element, the 2D-1D benchmark test case (rectangular cavity and elastic beam) is numerically solved as a 3D-2D case (cuboidal cavity and elastic plate), Figure 5(right) and the numerical results from the central plane section are compared to the aproximate analytical solution. Both the analytical and the numerical solution of the vibro-acoustic problem is provided for the cavity domain with dimensions $a = 1\,\text{m}$, $b = 2\,\text{m}$ and the amplitude $A_0 = 0.001\,\text{m s}^{-1}$ of the prescribed normal velocity at boundary Γ_{in}, Figure 4. In the numerical model, the third dimension is given as $z = 0.1\,\text{m}$. The air density is $\varrho_a = 1.177\,\text{kg m}^{-3}$ and the speed of sound is $c = 340\,\text{m s}^{-1}$. The elastic beam with thickness $h = 0.001\,\text{m}$, density $\varrho_h = 7800\,\text{kg m}^{-3}$, Young modulus $E = 2.1 \times 10^{11}\,\text{Pa}$ and Poisson ratio $\mu = 0.3$ is applied. The angular frequency $\omega = 50\,\text{rad s}^{-1}$ and proportional damping coefficient $\beta = 0$ are considered. Comparison of analytically and numerically computed absolute values of elastic beam/plate deflection amplitudes is provided in Figure 5(left). A minor deviations of the two solutions can be observed. These are likely caused by a limited number of harmonic functions respected in the approximate analytical solution (the provided solution refers to $N = 8$). For higher number of harmonics the problem becomes ill-conditioned. This is actually an advantage of numerical solution by means of FE method. Figure 5(right) displays a complete numerical solution of the vibro-acoustic problem. Both distribution of acoustic pressure amplitudes in the cavity domain and absolute values of deflection amplitudes at elastic plate. For completeness, there is a comparison of acoustic pressure amplitudes in the cavity as computed using approximate analytical solution, Figure 6(left), and numerically, Figure 6(right), showing a good agreement of the two solutions.

The second case studied numerically is a simplified model of mobile screw compressor. The compressor cavity is represented by a cuboidal computational domain geometry with dimensions $1000 \times 500 \times 700\,\text{mm}$ as depicted in Figure 7(top-left). The cavity bottom is rigid and corresponds to the boundary Γ_w. All other walls of the cuboidal domain form the interface
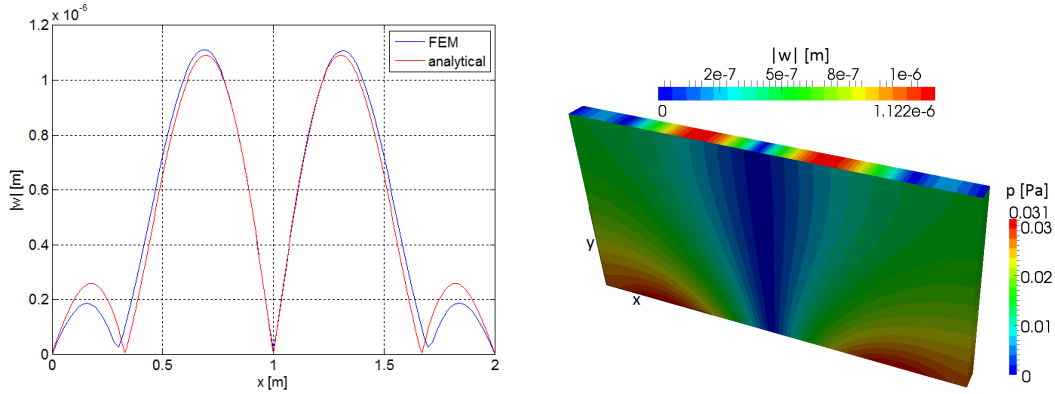
Figure 5: Benchmark test case: comparison of analytical (red) and numerical (blue) solution of absolute values of elastic beam/plate deflection amplitudes (left) and numerical solution of distribution of acoustic pressure amplitudes in cavity and of absolute values of deflection amplitudes at elastic plate (right).
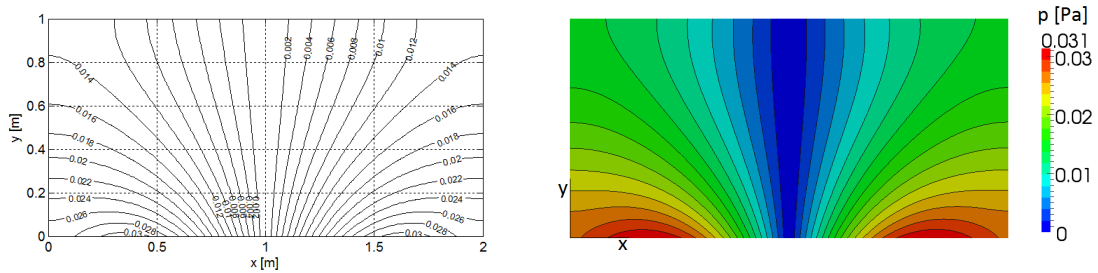

Figure 6: Benchmark test case: distribution of acoustic pressure amplitudes in cavity - approximate analytical solution (left) and numerical results (right).

boundary Γ_t between the compressor cavity and elastic housing. The elastic compressor housing is made of a thin metal plate with thickness $h = 0.001\,\mathrm{m}$ and density $\varrho_h = 7800\,\mathrm{kg\,m^{-3}}$. The compressor engine body is modelled as a small block attached to the rigid bottom and its surface represents the Γ_{in} boundary. The engine block dimensions are $400 \times 300 \times 300\,\mathrm{mm}$ and the prescribed amplitudes of normal velocity v_n are equal to $0.2249\,\mathrm{m\,s^{-1}}$. The following two parameters are selected: angular frequency of compressor engine motion $\omega = 200\,\mathrm{rad\,s^{-1}}$ and the coefficient of proportional damping $\beta = 0$. All other parameter values are identical to values from the previous benchmark test case. In Figure 7(right), the resulting distribution of the acoustic pressure amplitudes in the cavity of the simplified model of the screw compressor as solved by the implemented 3D FE solver is shown. Figure 7(bottom-left) displays absolute values of deflection amplitudes at compressor housing in a direction that is normal to the compressor housing surface.

The numerical results of a vibro-acoustic problem solved for a real geometry of the computational domain prepared according to the technical drawings provided by compressor producer and consisting of the engine body, the inner cavity and compressor housing will be presented during the conference ICOVP-2013.

6   CONCLUSIONS

The in-house 3D FE solver for vibro-acoustic analysis of screw compressors has been developed and the new 6-noded flat shell triangular finite element with 18 DOF implemented. Correctness of the proposed method and of the implemented solver has been verified using the benchmark test case, for which the analytical solution has been derived. First numerical results of vibro-acoustic analysis have been presented for a simplified screw compressor model. In
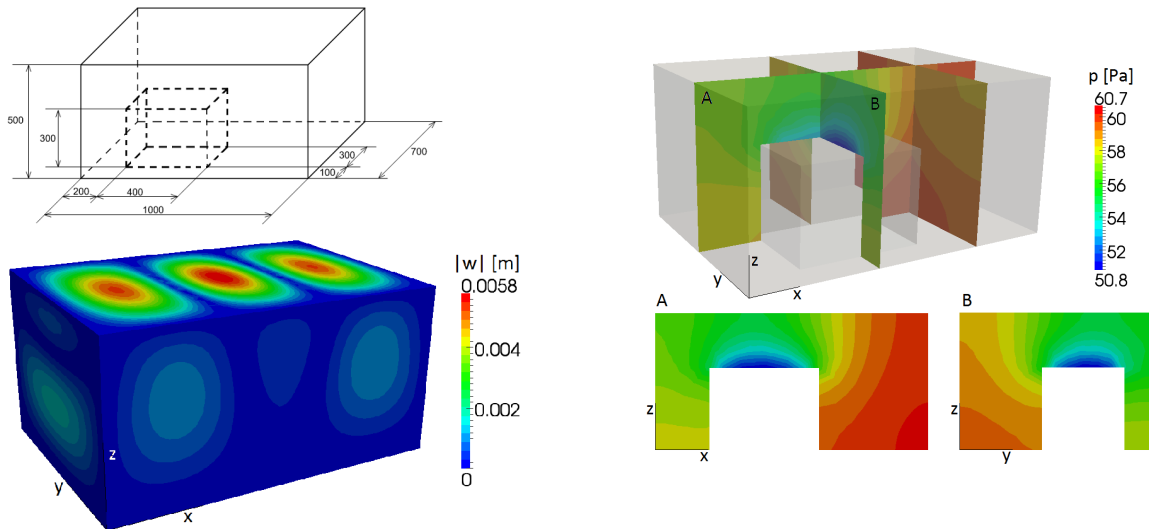
Figure 7: Simplified screw compressor model: computational domain geometry (top-left), numerical solution of absolute values of deflection amplitudes at compressor housing (bottom-let) and numerical solution of distribution of acoustic pressure amplitudes in compressor cavity (right).

order to quantify the total emitted acoustic power, the numerical solution in amplitude form has to be performed for all angular frequencies of periodically varying surface velocity of the compressor engine. Then the total emitted acoustic power is a superposition of all particular solutions. In the near future, the solution of compressor housing vibrations that are kinematically excited by the rotating parts of the screw compressor will be addressed and superimposed to the housing vibrations caused by the acoustic pressure field. The results of this numerical analysis will enable modifications of the present mobile screw compressor design which will lead to significant decrease in the total emitted acoustic power.

7 ACKNOWLEDGEMENTS

REFERENCES

[1] L.E. Kinsler, A.R. Frey, A.B. Coppens, J.V. Sanders, *Fundamentals of acoustics*. John Wiley & Sons, Inc., Forth eddition, 2000.

[2] S. Temkin, *Elements of acoustics*. Acoustical Society of America, 2001.

[3] P.M. Morse, K.U. Ingard, *Theoretical acoustics*. Princeton University Press, New Jersey, 1986.

[4] R. Matas, J. Kňourek, J. Voldřich, Influence of the terminal muffler geometry with three chambers and two tailpipes topology on its attenuation characteristics. *Applied and Computational Mechanics*, **3**, 121–132, 2009.

[5] A. Bermúdez, P. Gamallo, R. Rodríguez, Finite element methods in local active control of sound. *SIAM Journal on Control and Optimization*, **43**, 437–465, 2004.